DOI: 10.15825/1995-1191-2024-4-201-211

NUMERICAL ASSESSMENT OF THE EFFECT OF XENOPERICARDIAL BIOPROSTHETIC HEART VALVE CALCIFICATIONS ON ITS BIOMECHANICS

P.S. Onishchenko[1], K.Yu. Klyshnikov[1], A.A. Khromov[2], A.E. Kostyunin[1], T.V. Glushkova[1], T.N. Akentieva[1], E.A. Ovcharenko[1]

[1] Research Institute for Complex Issues of Cardiovascular Diseases, Kemerovo, Russian Federation
[2] Kuzbass Cardiology Center, Kemerovo, Russian Federation

Objective: to conduct a pilot study of the effect of bioprosthetic heart valve leaflet calcification on biomechanics and to identify the "stress in the material – dysfunction" relationship. **Materials and methods.** The study's focus was on two commercially available UniLine bioprosthetic mitral valves sized 26 and 30 (NeoCor, Russia). The samples were subjected to microcomputer tomographic scanning in order to reconstruct calcium volumes. The resulting 3D models were correlated with prostheses of corresponding sizes and projected to the volume of the locking element in the Abaqus/CAE engineering analysis software (Dassault Systemes, France). **Results.** According to numerical modeling, the maximum principal stresses increased significantly to 90.8 MPa in the samples, the opening decreased qualitatively, and impact on the prosthetic frame increased. Comparison of stress diagrams of numerical simulation with samples demonstrates the relationship between peak amplitude and rupture and thinning localizations in the flap apparatus. **Conclusion.** The work presented demonstrated the findings of a pilot study of the connection between biomechanics in a patient-specific calcified mitral prosthetic heart valve UniLine and macroscopic characterization of explanted samples. The comparative stage showed that stress values correlate with localization of leaflet dysfunction.

Keywords: bioprosthetic heart valves, calcification, dysfunctions, numerical modeling, biomechanics.

INTRODUCTION

According to various sources, over 9,000 heart valve surgeries are performed annually in the Russian Federation, with bioprosthetic heart valves (BHVs) accounting for at least 19% of these procedures [1]. BHVs offer several advantages over mechanical valves, including the absence of a need for lifelong anticoagulant therapy and the ability to more closely replicate native hemodynamics due to the design and materials of the leaflet components [2–4]. However, more than 30% of BHVs require replacement within 10–15 years due to various dysfunctions, such as calcification, pannus formation, ruptures, and perforations [5]. This highlights the need to investigate the underlying mechanisms [6–8] and develop preventive strategies [8, 9] for degenerative changes in the biological tissues of prosthetic valve leaflets. The main research approaches to addressing bioprosthetic valve dysfunction include:

– imaging techniques (X-ray, computed tomography (CT), micro-CT) [10–12];
– histological analysis [13–16];
– immunohistochemistry and immunofluorescence [16–19];
– blotting and proteomic profiling [20–22];
– sequencing [23–25];
– scanning electron microscopy [16, 26, 27].

Most of the aforementioned methods are now integrated in contemporary research, enabling a comprehensive characterization of valve dysfunction, including tissue destruction, cellular and bacterial infiltration, and protein deposition. With the advancement of computer simulation technologies, biomechanical analysis of prosthetic heart valves – both at the level of individual components and the prosthesis as a whole – has become increasingly feasible [28–33]. A major focus of current research is the evaluation of the stress-strain state of the leaflet material and the progression of valve dysfunction over time [32–35].

Initial studies in valve biomechanics modeled the leaflet structure using shell-based approaches, where the material's thickness was a key parameter [28, 34]. More recent efforts have shifted toward volumetric modeling [32], which allows for more accurate representation of *in situ* mechanical behavior. Similarly, calcific deposits can be incorporated either as material properties within the computational mesh [28] or explicitly represented as three-dimensional bodies on the valve surface [32, 34]. However, literature evidence suggests that such degene-

Corresponding author: Pavel Onishchenko. Address: 6, Barbarash boulevard, Kemerovo, 650002, Russian Federation. Phone: (3842) 34-55-86. E-mail: onis.pavel@gmail.com

rative changes may also localize within the thickness of the leaflet tissue itself [36–39]. This highlights a notable limitation in current modeling approaches – the oversimplified mathematical representation of the structural complexities within the leaflet tissue.

To address the shortcomings identified in previous numerical modeling studies of BHV dysfunction, we developed a novel approach for conducting in silico experiments. This method was validated through a comparative analysis involving both an intact (initial) model and a patient-specific model of a BHV. Additionally, the numerical modeling results were compared against dysfunctions observed in explanted xenopericardial mitral prostheses.

MATERIALS AND METHODS

The study focused on two UniLine bioprosthetic mitral valves (NeoCor, Russia) [40, 41], with diameters of 26 mm and 30 mm (Fig. 1, a), which were electively explanted due to dysfunction after 4.3 and 5.3 years of *in vivo* use, respectively. Within four hours of explantation, photographic documentation of the dysfunctional regions was performed, followed by detailed macroscopic imaging to facilitate comparison with biomechanical simulation outcomes.

Subsequently, both specimens underwent microcomputed tomography using a previously established protocol [27]. The acquired tomographic slices were imported into the Mimics medical 3D engineering software (Materialise, Belgium), where volumetric models of calcific lesions (Fig. 1, b) were reconstructed based on radiodense regions, as described in earlier methodologies [42].

Subsequently, we developed a computational model within the Abaqus engineering analysis environment

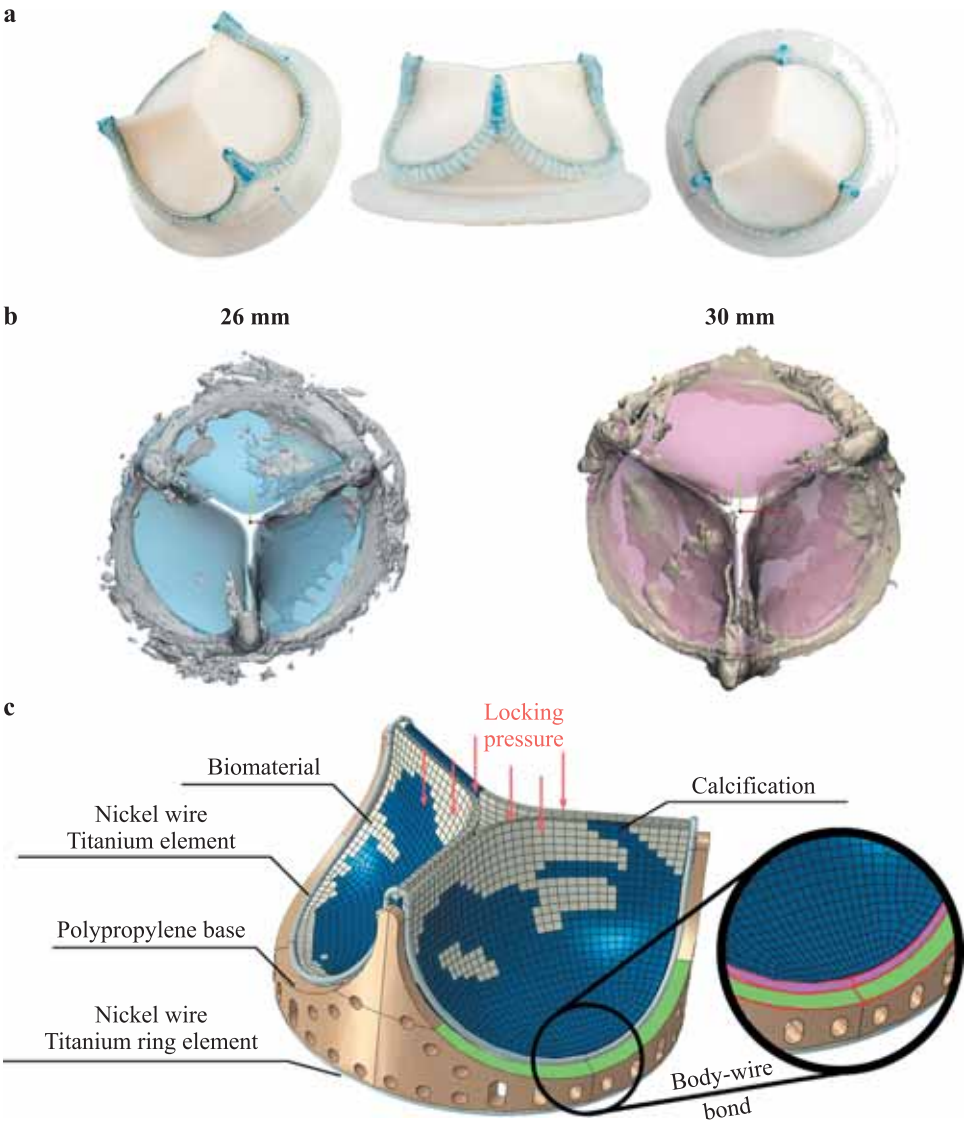

Fig. 1. UniLine bioprosthetic mitral valve: a, general view; b, comparison of the prosthesis model and calcifications reconstructed from micro-CT; c, description of the assembly components, visualization of applied pressure and interaction of the pairs of elements

(Dassault Systèmes, France), using the Dynamic/Explicit solver. The 3D model of the bioprosthesis, which included polypropylene and wire support structures along with 3 valve cusps (Fig. 1, b), was augmented with volumetric representations of calcifications (Fig. 2, b). A 3D finite element mesh was then constructed, comprising C3D8 hexahedral solid elements for the polypropylene frame and leaflet apparatus, and C3D4 tetrahedral elements for the wire components fabricated from titanium nickelide. The final meshes contained 15,862 and 21,031 elements for the 26 mm and 30 mm prostheses, respectively.

The biomechanical performance of the leaflet apparatus, including calcified regions, was assessed by simulating 2 complete cardiac cycles at a heart rate of 70 beats per minute, spanning a total simulation time of 0–1.8 seconds. Material properties were assigned in accordance with manufacturer specifications [43] and previously published data [44, 45]. Calcified regions were modeled as rigid bodies, following standard parameters for calcium deposits [44].

Uniaxial tensile test data for the leaflet material [46] were imported into the Abaqus/CAE environment, where coefficients were fitted for a nonlinear constitutive model (Table) using the following strain energy function:

$$W = \sum_{i=0}^{n} C_{i0}(I_1 - 3)^i,$$

where W is strain energy density, C_{i0} is Rivlin coefficient, and I_1 is first invariant of Green deformation tensor.

Table

Coefficients of the nonlinear biomaterial model

C_{10}, MPa	C_{20}, MPa	C_{30}, MPa	C_{40}, MPa
0.0071	0.5036	1.023	–0.651

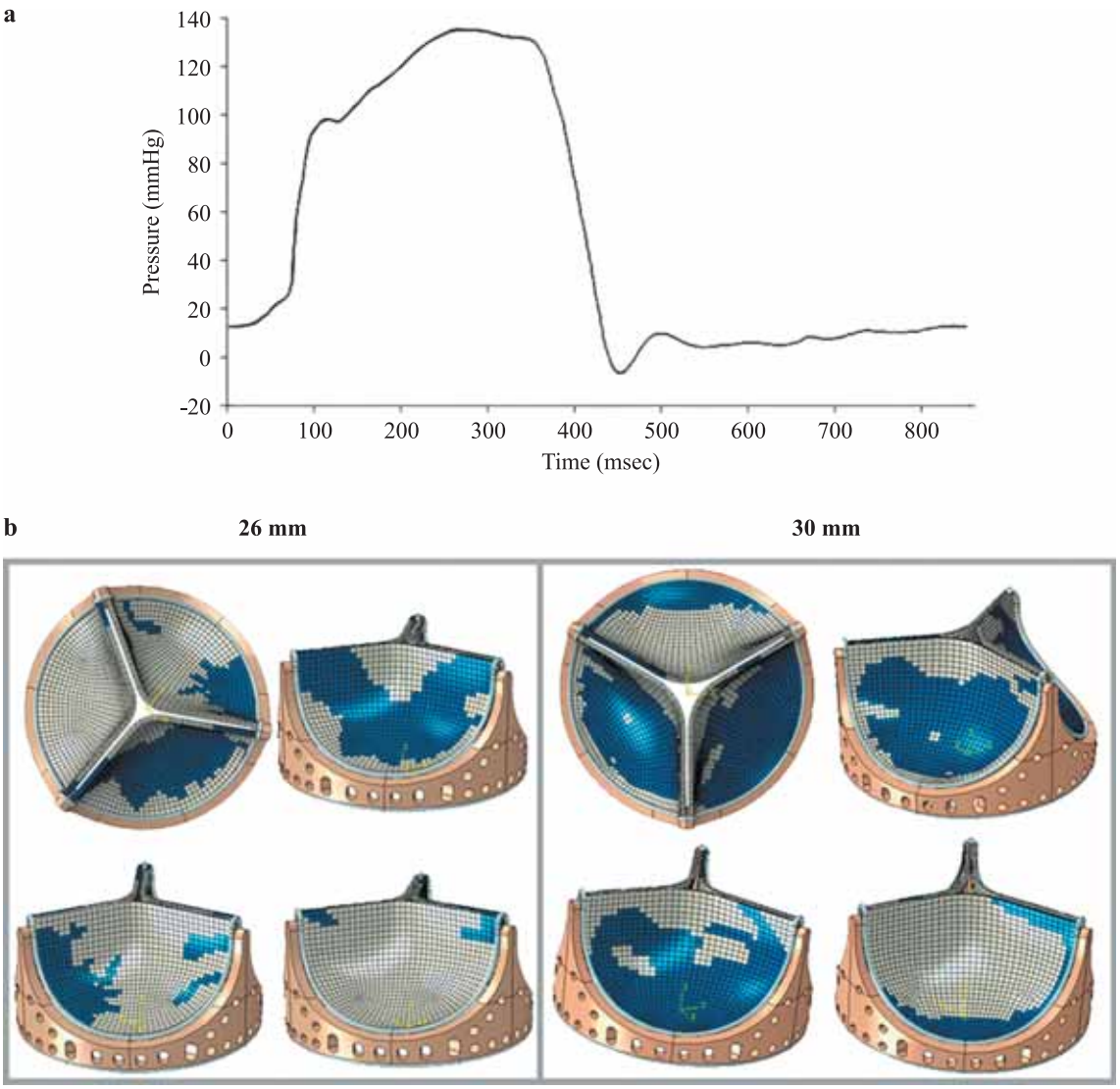

Fig. 2. Modeling methodology: a, pressure applied to the valve plug; b, location of calcifications (blue) in the biomaterial of the flap apparatus (gray)

Contact between the valve leaflets was modeled using a "hard contact" interaction with a coefficient of friction set at 0.2. All components of the prosthesis were integrated into a unified assembly via paired tie-type constraints: specifically, between the nodes of the polypropylene frame and the wire components, as well as between the upper wire component and the lower suture edge of the leaflet. Boundary conditions enforcing complete fixation – zero displacement and zero rotation – were applied to the lower annular wire component (Fig. 1, b). Hemodynamic loading was simulated by applying physiological pressure to the leaflet surface from the left ventricular side (Fig. 2, a, Fig. 1, b).

For comparison, UniLine valve models without calcification – featuring leaflets composed of a homogeneous xenopericardial material – were also simulated under identical conditions. In all modeled cases, the maximum principal stress was used as the key quantitative indicator to evaluate leaflet biomechanics.

RESULTS

Modeling of prosthetic biomechanics with no degenerative changes

At this stage, simulations were performed on BHV models in their intact state, without calcification of the leaflet apparatus. The results are presented in Fig. 3.

The analysis revealed increased stress concentrations at the commissural strut regions, with a uniform stress distribution throughout the volume of the polypropylene frame and symmetrical loading of the leaflet apparatus onto the wire component. During the entire cardiac cycle, peak stress did not exceed 11.5 MPa for the 26 mm prosthesis and 16.5 MPa for the 30 mm prosthesis. These values remain well below the threshold for irreversible deformation of the leaflet material [44, 47].

Modeling considering calcium deposits in the leaflet apparatus

The inclusion of leaflet calcification in the computational model significantly altered the biomechanical behavior of the bioprosthesis. Notably, there was a marked increase in peak maximum principal stress, accompanied by a qualitative reduction in leaflet opening amplitude (Fig. 4).

The most pronounced biomechanical changes were observed in the 26 mm UniLine bioprosthesis model. Peak maximum principal stresses within the calcified regions ranged from 30.5 MPa to 48.8 MPa, predominantly localized at sites of interaction with the wire frame. These elevated stress values are attributed to material stretching during the valve closure phase, with stress amplitudes reducing to an average of 20 MPa during valve opening.

Interestingly, larger-volume calcific deposits exhibited lower peak stress magnitudes compared to smaller clusters – 30 MPa in the closed state versus 6.3 MPa during opening. In addition, both the polypropylene base and wireframe elements experienced significantly increased loading compared to their intact counterparts.

The UniLine bioprosthesis with a 30 mm diameter, due to the greater volume of biomaterial in its leaflet structure, exhibited a more uniform stress distribution compared to the 26 mm model. However, maximum principal stresses in this model remained substantially elevated relative to the intact condition, reaching up to 90.8 MPa during closure and 55.9 MPa in the opening

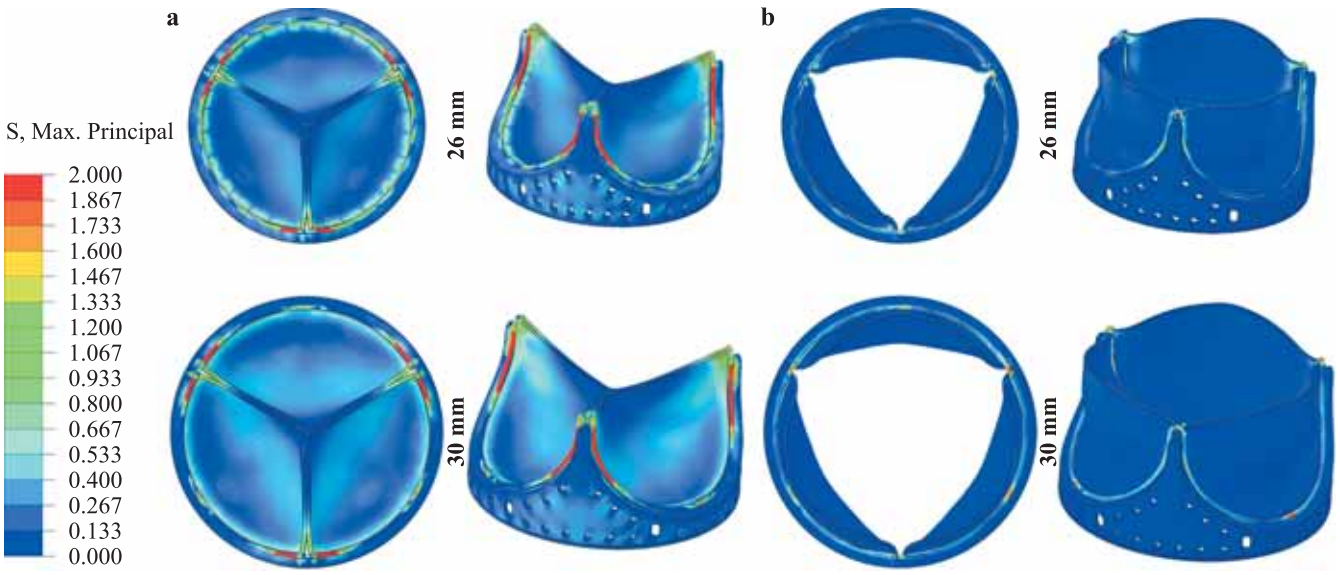

Fig. 3. Results of numerical modeling of the UniLine bioprosthetic valve of 26 mm (top row) and 30 mm (bottom row) diameter in an intact state at a: closure, T = 1.188 sec; b: maximum opening, T = 1.584 sec

phase, particularly in the region of the leaflet's free edge. There were no significant alterations in the stress experienced by the polypropylene framework component.

Correlation between biomechanical simulation and explanted bioprosthesis specimens

At this stage, we addressed a key question: to what extent do the simulated calcification zones within the leaflet apparatus, and the associated localized stress concentrations (Fig. 5, b, c), correlate with the structural dysfunctions observed in the explanted prostheses (Fig. 5, a)?

The study reveals irregularities and steep gradients in stress magnitude, which correspond to areas of tissue thinning (Fig. 5, b, c) and leaflet tears (Fig. 5, c). These changes are predominantly localized in the commissural regions, suggesting that mechanical stretching plays a critical role in the pathogenesis of structural degeneration.

One plausible mechanism underlying this dysfunction is the abrasion and subsequent disruption of the surface layer of the leaflet tissue at its attachment to the wireframe component. This disruption likely facilitates calcium penetration into the locking element.

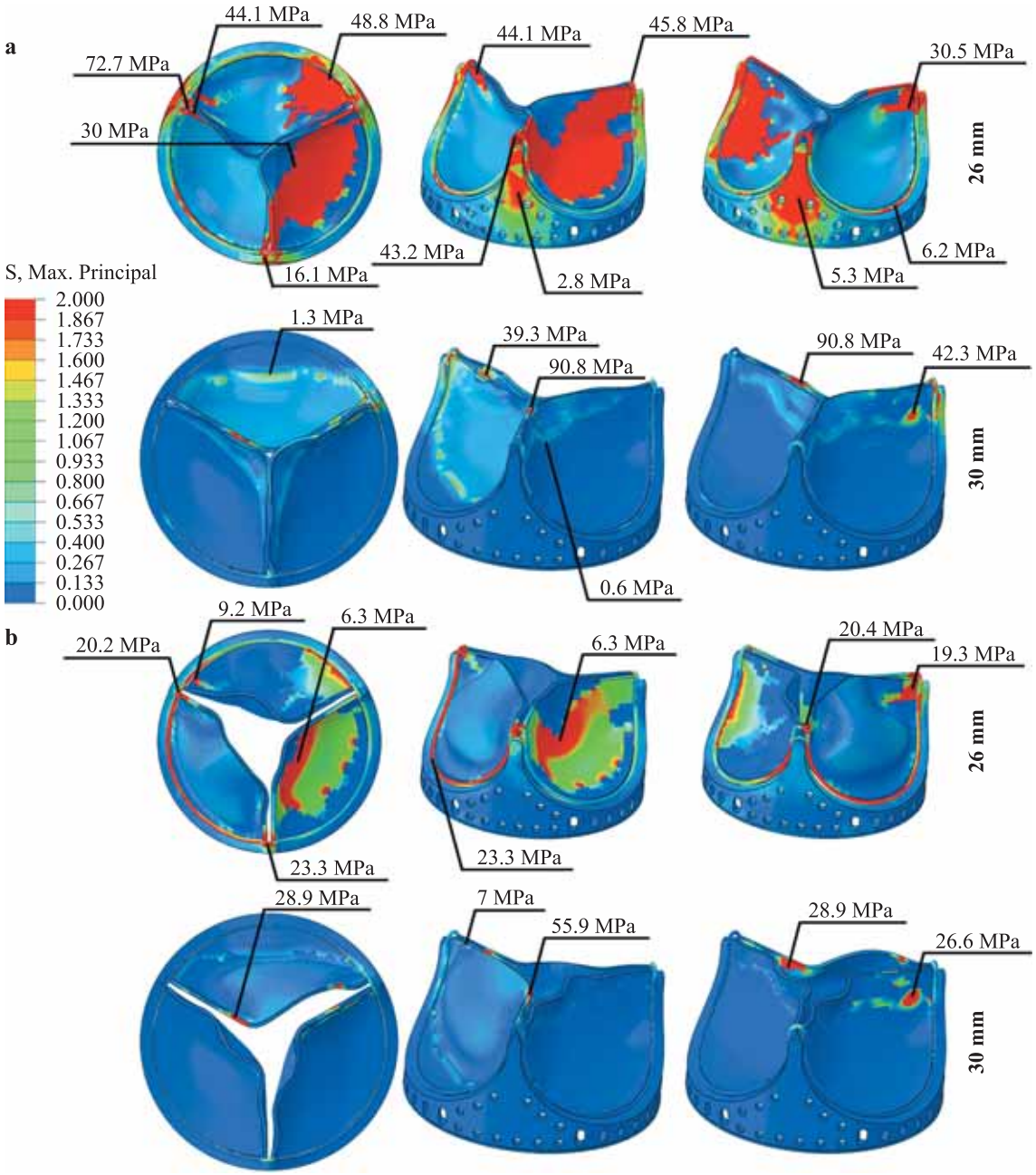

Fig. 4. Results of numerical modeling of the biomechanics of the UniLine bioprosthetic mitral valve with a diameter of 26 and 30 mm in a: closed state, T = 1.188 sec; b: open state, T = 1.584 sec

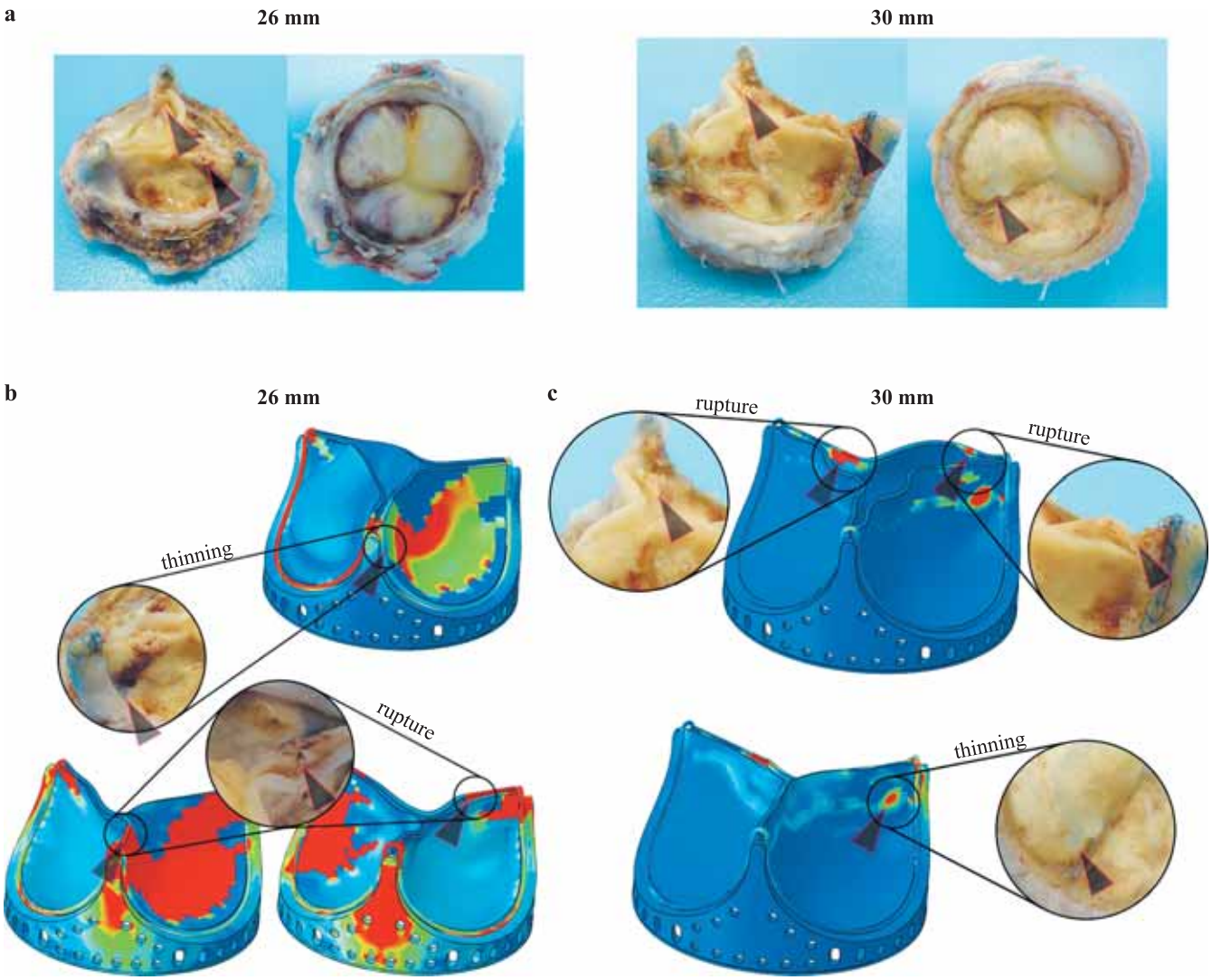

Fig. 5. Comparison of excised samples (a) and comparison of dysfunction areas with modeling results of the UniLine bioprosthetic valves of diameter 26 mm (b) and 30 mm (c). The corresponding comparison areas are highlighted with translucent pointers. The coloring of the diagrams corresponds to the scale of maximum principal stress [0, 2] MPa

DISCUSSION

On one hand, various research groups have demonstrated the significant impact of structural alterations on the performance of artificial heart valve substitutes. Hamid et al. (1987) [28] examined how the location of calcium deposits and the presence of perforations influence the vibrational behavior of the leaflet dome. Given the limited computational resources available at the time, the authors focused on estimating the fundamental natural frequency – a key parameter in assessing the mechanical stability and durability of BHVs. Their findings indicated that a central perforation reduced the natural frequency from 55 Hz (in a native, healthy valve) to 52 Hz. Inclusion of calcifications increased the frequency to 62 Hz, while damage involving all three leaflets caused a dramatic rise to 145 Hz.

With advancements in hardware and computing performance, more sophisticated simulations have become possible. In 2016, for instance, researchers presented a model simulating the implantation of a balloon-expandable prosthesis into a calcified native valve, using the commercial Edwards SAPIEN valve (Edwards Lifesciences Inc., USA) as a reference [34]. The study presents detailed stress distribution patterns and analyzes the biomechanical behavior of the leaflet apparatus as influenced by the implantation technique of the prosthesis. The findings demonstrate that stress amplitudes increase notably in regions with calcium accumulations, with the first principal stress component (σ_1) exceeding 0.5 MPa. In contrast, areas with an intact (“clean”) surface exhibit much lower stress, typically below 0.15 MPa. Further advancement of this modeling approach was presented by Qin et al. in 2020 [32], who investigated stenotic heart valves using patient-specific native valve models. Their study revealed a strong correlation between stress distribution and location of calcifications. Stress concent-

rations were localized at the interface between the leaflet dome and the calcified regions. Quantitative analysis indicated an average increase in stress amplitudes by about 1.4 ± 0.08 times compared to non-calcified models, depending on the extent of the lesion.

On the other hand, numerous histological studies involving both animal models and explanted BHVs have documented structural deterioration characterized by calcium deposits surrounded by a disrupted cellular matrix [36–39]. Microscopic examination of affected tissues reveals detachment of collagen fibers from the mineralized inclusions, a phenomenon attributed to repetitive mechanical impact during the cardiac cycle. This process is believed to underlie the development of ruptures and perforations in BHVs.

A similar observation was made in this study, where regions of tissue thinning and tearing in the excised bioprosthetic specimens corresponded with zones of elevated mechanical stress. The findings underscore the substantial impact of leaflet calcification on the biomechanical performance of the prosthesis. Specifically, calcific deposits markedly alter the distribution and magnitude of maximum principal stresses, thereby impairing the leaflet's ability to reproduce native hemodynamics. The two case studies presented here effectively illustrate the potential relationship between stress concentration and valve dysfunction. However, to establish more generalizable conclusions and to validate these findings, a multicenter study is warranted. Such a study should integrate advanced noninvasive imaging and calcium mapping techniques for biomechanical modeling, alongside modern immunophenotyping approaches. The methodology presented here demonstrates the feasibility of conducting pilot investigations using explanted samples, laying the groundwork for larger-scale research initiatives.

CONCLUSIONS

The biomechanical impact of calcification within the leaflet apparatus on stress distribution in both the supporting frame and the dome of the cusps was investigated using two UniLine bioprosthetic valves (26 mm and 30 mm in diameter) explanted due to structural degeneration. The analysis revealed a marked increase in peak stress amplitudes – reaching up to 90.8 MPa – in regions containing calcium deposits. These elevated stress concentrations negatively affected the surrounding tissue integrity, contributing to leaflet thinning and rupture. Furthermore, in the 26 mm UniLine valve, structural modeling that incorporated calcifications demonstrated increased mechanical loading on both the wire support elements and the polypropylene frame component.

This work was conducted as part of the fundamental research project of the Research Institute for Complex Issues of Cardiovascular Diseases, titled "Molecular, cellular, and biomechanical mechanisms of the pathogenesis of cardiovascular diseases in the development of new treatment methods based on personalized pharmacotherapy, the introduction of minimally invasive medical devices, biomaterials, and tissue-engineered implants" (Research Supervisor: Professor Leonid Barbarash, Fellow, Russian Academy of Sciences), subject code 0419-2022-0001.

The authors express their sincere gratitude for the support provided within the framework of the project "Foundation for Support of Young Scientists in Biomedical Sciences", and especially thank Professor E.V. Grigoriev (MD), Fellow, Russian Academy of Sciences, for his valuable assistance and guidance.

The authors declare no conflict of interest.

REFERENCES

1. *Bokeria LA, Milievskaya EB, Kudzoeva ZF, Pryanishnikov BB, Skopin AI, Yurlov IA.* Cardiovascular Surgery – 2018. Diseases and congenital anomalies of the circulatory system. Moscow, 2018; 270.
2. *Bonow RO, O'Gara PT, Adams DH, Badhwar V, Bavaria JE, Elmariah S et al.* 2020 Focused Update of the 2017 ACC Expert Consensus Decision Pathway on the Management of Mitral Regurgitation: A Report of the American College of Cardiology Solution Set Oversight Committee. *J Am Coll Cardiol [Internet]*. 2020 May 5 [cited 2023 May 26]; 75 (17): 2236–2270. Available from: https://pubmed.ncbi.nlm.nih.gov/32068084/.
3. *Nishimura RA, Otto CM, Bonow RO, Carabello BA, Erwin JP, Fleisher LA et al.* 2017 AHA/ACC Focused Update of the 2014 AHA/ACC Guideline for the Management of Patients with Valvular Heart Disease: A Report of the American College of Cardiology / American Heart Association Task Force on Clinical Practice Guidelines. *Circulation [Internet]*. 2017 Jun 20 [cited 2023 May 26]; 135 (25): e1159–e1195. Available from: https://www.ahajournals.org/doi/abs/10.1161/CIR.0000000000000503.
4. *Marom G, Einav S.* New insights into valve hemodynamics. *Rambam Maimonides Med J*. 2020 Apr 29; 11 (2): e0014. doi: 10.5041/RMMJ.10400.
5. *Velho TR, Pereira RM, Fernandes F, Guerra NC, Ferreira R, Nobre Â.* Bioprosthetic Aortic Valve Degeneration: a Review from a Basic Science Perspective. *Brazilian J Cardiovasc Surg*. 2022; 37 (2): 239–250. doi: 10.21470/1678-9741-2020-0635.

6. *Brockbank KGM, Song YC.* Mechanisms of bioprosthetic heart valve calcification. *Transplantation*. 2003; 75 (8): 1133–1135. doi: 10.1097/01.TP.0000062864.54455.E5.
7. *Scott Rapoport H, Connolly JM, Fulmer J, Dai N, Murti BH, Gorman RC et al.* Mechanisms of the *in vivo* inhibition of calcification of bioprosthetic porcine aortic valve cusps and aortic wall with triglycidylamine/mercapto bisphosphonate. *Biomaterials*. 2007; 28 (4): 690–699. doi: 10.1016/j.biomaterials.2006.09.029.
8. *Wen S, Zhou Y, Yim WY, Wang S, Xu L, Shi J et al.* Mechanisms and Drug Therapies of Bioprosthetic Heart Valve Calcification. *Front Pharmacol*. 2022 Jun 3; 13: 909801. doi: 10.3389/fphar.2022.909801.
9. *Timchenko TP.* Bisphosphonates as Potential Inhibitors of Calcification in Bioprosthetic Heart Valves (Review). *Modern Technologies in Medicine*. 2022; 14 (2): 68–79. doi: 10.17691/stm2022.14.2.07.
10. *Alwan L, Bernhard B, Brugger N, de Marchi SF, Praz F, Windecker S et al.* Imaging of Bioprosthetic Valve Dysfunction after Transcatheter Aortic Valve Implantation. *Diagnostics (Basel)*. 2023 May 29; 13 (11): 1908. doi: 10.3390/diagnostics13111908.
11. *Piérard S, Seldrum S, Muller T, Gerber BL.* Evaluation of aortic bioprosthesis stenosis by multidetector CT. *J Cardiovasc Comput Tomogr*. 2012; 6 (1): 62–65. doi: 10.1016/j.jcct.2011.11.005.
12. *Cartlidge TRG, Doris MK, Sellers SL, Pawade TA, White AC, Pessotto R et al.* Detection and Prediction of Bioprosthetic Aortic Valve Degeneration. *J Am Coll Cardiol*. 2019; 73 (10): 1107–1119. doi: 10.1016/j.jacc.2018.12.056.
13. *Lepidi H, Casalta JP, Fournier PE, Habib G, Collart F, Raoult D.* Quantitative histological examination of mechanical heart valves. *Clin Infect Dis*. 2005; 40 (5): 655–661. doi: 10.1086/427504.
14. *Sellers SL, Turner CT, Sathananthan J, Cartlidge TRG, Sin F, Bouchareb R et al.* Transcatheter Aortic Heart Valves: Histological Analysis Providing Insight to Leaflet Thickening and Structural Valve Degeneration. *JACC Cardiovasc Imaging*. 2019; 12 (1): 135–145. doi: 10.1016/j.jcmg.2018.06.028.
15. *Lepidi H, Casalta JP, Fournier PE, Habib G, Collart F, Raoult D.* Quantitative histological examination of bioprosthetic heart valves. *Clin Infect Dis*. 2006; 42 (5): 590–596. doi: 10.1086/500135.
16. *Prokudina ES, Senokosova EA, Antonova LV, Muhamadijarov RA, Koshelev VA, Krivkina EO et al.* Morphological features of biological and tissue-engineered vascular patches remodeling: results of tests on a sheep model. *The Siberian Journal of Clinical and Experimental Medicine*. 2023; 38 (4): 250–259. [In Russ., English abstact]. doi: 10.29001/2073-8552-2023-38-4-250-259.
17. *Bogdanov LA, Velikanova EA, Shishkova DK, Shabaev AR, Kutikhin AG.* Neointimal remodeling in carotid atherosclerosis: roles of matrix metalloproteinases-2 and -9 and different phenotypes of vascular smooth muscle cells. *Pathological physiology and experimental therapy*. 2020; (4): 20–30. [In Russ, English abstract]. doi: 10.25557/0031-2991.2020.04.20-30.
18. *Human P, Bezuidenhout D, Aikawa E, Zilla P.* Residual Bioprosthetic Valve Immunogenicity: Forgotten, Not Lost. *Front Cardiovasc Med*. 2022 Jan 4; 8: 760635. doi: 10.3389/fcvm.2021.760635.
19. *Marro M, Kossar AP, Xue Y, Frasca A, Levy RJ, Ferrari G.* Noncalcific mechanisms of bioprosthetic structural valve degeneration. *J Am Heart Assoc*. 2021; 10 (3): 1–13. doi: 10.1161/JAHA.120.018921.
20. *Shishkova DK, Glushkova TV, Efimova OS, Popova AN, Malysheva VY, Kolmykov RP et al.* Morphological and Chemical Properties of Spherical and Needle Calcium Phosphate Bions. *Complex Issues Cardiovasc Dis*. 2019; 8 (1): 59–69. doi: 10.17802/2306-1278-2019-8-1-59-69.
21. *Abramov A, Xue Y, Zakharchenko A, Kurade M, Soni RK, Levy RJ, Ferrari G.* Bioprosthetic heart valve structural degeneration associated with metabolic syndrome: Mitigation with polyoxazoline modification. *Proc Natl Acad Sci USA*. 2023 Jan 3; 120 (1): e2219054120. doi: 10.1073/pnas.2219054120.
22. *Smart I, Goecke T, Ramm R, Petersen B, Lenz D, Haverich A et al.* Dot blots of solubilized extracellular matrix allow quantification of human antibodies bound to epitopes present in decellularized porcine pulmonary heart valves. *Xenotransplantation*. 2021; 28 (1). doi: 10.1111/xen.12646.
23. *Asanov MA, Kazachek YV, Evtushenko AV, Teplova YE, Ponasenko AV.* Comparison of Microflora Isolated From Peripheral Blood and Valvular Structures of the Heart in Patients With Infective Endocarditis. *Acta Biomed Sci*. 2022; 7 (2): 91–98. doi: 10.29413/ABS.2022-7.2.10.
24. *Mohammadi MM, Bavi O.* DNA sequencing: an overview of solid-state and biological nanopore-based methods. *Biophys Rev*. 2022; 14 (1): 99–110. doi: 10.1007/s12551-021-00857-y.
25. *Rovery C, Greub G, Lepidi H, Casalta JP, Habib G, Collart F, Raoult D.* PCR detection of bacteria on cardiac valves of patients with treated bacterial endocarditis. *J Clin Microbiol*. 2005; 43 (1): 163–167. doi: 10.1128/JCM.43.1.163-167.2005.
26. *Mukhamadiyarov RA, Bogdanov LA, Glushkova TV, Shishkova DK, Kostyunin AE, Koshelev VA et al.* Embedding and backscattered scanning electron microscopy: A detailed protocol for the whole-specimen, high-resolution analysis of cardiovascular tissues. *Front Cardiovasc Med*. 2021 Oct 25; 8: 73954. doi: 10.3389/fcvm.2021.739549.
27. *Keklikoglou K, Arvanitidis C, Chatzigeorgiou G, Chatzinikolaou E, Karagiannidis E, Koletsa T et al.* Micro-CT for biological and biomedical studies: A comparison of imaging techniques. *J Imaging*. 2021 Sep 1; 7 (9): 172. doi: 10.3390/jimaging7090172.
28. *Hamid MS, Sabbah HN, Stein PD.* Vibrational analysis of bioprosthetic heart valve leaflets using numerical models: Effects of leaflet stiffening, calcification, and perfo-

ration. *Circ Res*. 1987; 61 (5): 687–694. doi: 10.1161/01.RES.61.5.687.
29. *Claiborne TE, Sheriff J, Kuetting M, Steinseifer U, Slepian MJ, Bluestein D. In vitro* evaluation of a novel hemodynamically optimized trileaflet polymeric prosthetic heart valve. *J Biomech Eng*. 2013 Feb; 135 (2): 021021. doi: 10.1115/1.4023235.
30. *Claiborne TE, Xenos M, Sheriff J, Chiu WC, Soares J, Alemu Y et al.* Toward optimization of a novel trileaflet polymeric prosthetic heart valve via device thrombogenicity emulation. *ASAIO J*. 2013; 59 (3): 275–283. doi: 10.1097/MAT.0b013e31828e4d80.
31. *Xuan Y, Dvir D, Wang Z, Mizoguchi T, Ye J, Guccione JM et al.* Stent and leaflet stresses in 26-mm, third-generation, balloon-expandable transcatheter aortic valve. *J Thorac Cardiovasc Surg*. 2019; 157 (2): 528–536. doi: 10.1016/j.jtcvs.2018.04.115.
32. *Qin T, Caballero A, Mao W, Barrett B, Kamioka N, Lerakis S, Sun W.* The role of stress concentration in calcified bicuspid aortic valve. *J R Soc Interface*. 2020 Jun; 17 (167): 20190893. doi: 10.1098/rsif.2019.0893.
33. *Kazik HB, Kandail HS, LaDisa JF, Lincoln J.* Molecular and Mechanical Mechanisms of Calcification Pathology Induced by Bicuspid Aortic Valve Abnormalities. *Front Cardiovasc Med*. 2021 May 26; 8: 677977. doi: 10.3389/fcvm.2021.677977.
34. *Sturla F, Ronzoni M, Vitali M, Dimasi A, Vismara R, Preston-Maher G et al.* Impact of different aortic valve calcification patterns on the outcome of transcatheter aortic valve implantation: A finite element study. *J Biomech*. 2016; 49 (12): 2520–2530. doi: 10.1016/j.jbiomech.2016.03.036.
35. *Weinberg EJ, Schoen FJ, Mofrad MRK.* A computational model of aging and calcification in the aortic heart valve. *PLoS One*. 2009 Jun 18; 4 (6): e5960. doi: 10.1371/journal.pone.0005960.
36. *Thubrikar MJ, Deck JD, Aouad J, Nolan SP.* Role of mechanical stress in calcification of aortic bioprosthetic valves. *J Thorac Cardiovasc Surg*. 1983; 86 (1): 115–125. doi: 10.1016/s0022-5223(19)39217-7.
37. *Van der Valk DC, Fomina A, Uiterwijk M, Hooijmans CR, Akiva A, Kluin J et al.* Calcification in Pulmonary Heart Valve Tissue Engineering: A Systematic Review and Meta-Analysis of Large-Animal Studies. *JACC Basic to Transl Sci*. 2023; 8 (5): 572–591. doi: 10.1016/j.jacbts.2022.09.009.
38. *Schoen FJ, Tsao JW, Levy RJ.* Calcification of bovine pericardium used in cardiac valve bioprostheses. *Am J Pathol*. 1986; 123: 134–145.
39. *Sakaue T, Koyama T, Nakamura Y, Okamoto K, Kawashima T, Umeno T et al.* Bioprosthetic Valve Deterioration: Accumulation of Circulating Proteins and Macrophages in the Valve Interstitium. *JACC Basic to Transl Sci*. 2023; 8 (7): 862–880. doi: 10.1016/j.jacbts.2023.01.003.
40. *Khalivopulo IK, Evtushenko AV, Shabaldin AV, Troshkinev NM, Stasev AN, Kokorin SG, Barbarash LS.* Comparison of Propensity Scores for Surgical Treatment of Bioprosthetic Mitral Valve Dysfunction Using Traditional and "Valve-in-Valve" Methods. *Complex Issues Cardiovasc Dis*. 2023; 12 (2): 57–69. doi: 10.17802/2306-1278-2023-12-2-57-69.
41. *Fedorov SA, Chiginev VA, Zhurko SA, Gamzaev AB, Medvedev AP.* Clinical and hemodynamic results of using different models of biological prostheses for correction of senile aortic valve malformations. *Modern Technologies in Medicine*. 2016; 8 (4): 292–296. (in Russ).
42. *Pestiaux C, Pyka G, Quirynen L, De Azevedo D, Vanoverschelde JL, Lengelé B et al.* 3D histopathology of stenotic aortic valve cusps using *ex vivo* microfocus computed tomography. *Front Cardiovasc Med*. 2023 Apr 25; 10: 1129990. doi: 10.3389/fcvm.2023.1129990.
43. ExxonMobil. Datasheet. 2022 [cited 2023 Jul 19]. p. 2 ExxonMobilTM PP1014H1 Polypropylene Homopolymer. Available from: https://exxonmobilchemical.ulprospector.com/datasheet.aspx.
44. *Finotello A, Gorla R, Brambilla N, Bedogni F, Auricchio F, Morganti S.* Finite element analysis of transcatheter aortic valve implantation: Insights on the modelling of self-expandable devices. *J Mech Behav Biomed Mater*. 2021 Nov; 123: 104772. doi: 10.1016/j.jmbbm.2021.104772.
45. *Capelli C, Bosi GM, Cerri E, Nordmeyer J, Odenwald T, Bonhoeffer P et al.* Patient-specific simulations of transcatheter aortic valve stent implantation. *Med Biol Eng Comput [Internet]*. 2012 Feb [cited 2022 Mar 16]; 50 (2): 183–192. Available from: https://pubmed.ncbi.nlm.nih.gov/22286953/.
46. *Onishchenko P, Glushkova T, Kostyunin A, Rezvova M, Akentyeva T, Barbarash L.* Computer models of biomaterials used for manufacture of flap apparatus of prosthetic heart valves. *Mater Sci*. 2023; 0 (7): 30–39. doi: 10.31044/1684-579x-2023-0-7-30-39.
47. *Guo S, Shi Y, Zhang H, Meng Q, Su R, Zhang J et al.* Design and fabrication of a Nb/NiTi superelastic composite with high critical stress for inducing martensitic transformation and large recoverable strain for biomedical applications. *Mater Sci Eng C Mater Biol Appl*. 2020 Jul; 112: 110894. doi: 10.1016/j.msec.2020.110894.

The article was submitted to the journal on 19.04.2024